Optics Communications 371 (2016) 173–177

Contents lists available at ScienceDirect

Optics Communications

journal homepage: www.elsevier.com/locate/optcom

Dual-band infrared perfect absorber for plasmonic sensor based on the electromagnetically induced reflection-like effect

Yang Liu [a], Ying Qiao Zhang [a,*], Xing Ri Jin [a,*], Shou Zhang [a], Young Pak Lee [b]

[a] Department of physics, College of Science, Yanbian University, Yanji, Jilin 133000, People's Republic of China
[b] Quantum Photonic Science Research Center and Department of Physics, Hanyang University, Seoul 133-791, Republic of Korea

ARTICLE INFO

Article history:
Received 24 January 2016
Received in revised form
17 March 2016
Accepted 22 March 2016

Keywords:
Metamaterials
Resonance
Surface plasmons
Optical devices

ABSTRACT

We present a scheme for realizing a narrow-dual-band perfect absorber based on the plasmonic analogy of the electromagnetically induced reflection (EIR)-like effect. In our scheme, two short gold bars are excited strongly by incident plane wave serving as the bright mode. The middle gold bar is excited by two short gold bars. Due to the strong hybridization between the two short gold bars and the middle gold bar, two absorption peaks occur. The corresponding absorption rates are both over 99%. The quality factors of the two absorption peaks are 41.76 (198.47 THz) and 71.42 (207.79 THz), respectively, and the narrow-distance of the two absorption peaks is 9.32 THz. Therefore, they are narrow enough for the absorber to be a filter and a dual-band plasmonic sensor.

Metamaterials are kinds of artificially fabricated materials engineered to exhibit extraordinary properties that are not achievable in natural materials and they have a wide range of applications, such as negative refraction [1], solar cells [2], bolometers [3], photodetectors [4,5], classical analogue of electromagnetically induced transparency [6–12] perfect absorbers [13–28,30–33], and so on. According to the classification of absorbing bandwidth, metamaterial perfect absorbers are divided into two categories, broad-band absorbers [16–21] and narrow-band absorbers [22–28,30,31]. The broad-band absorbers can be used for solar cell and light harvesting, and the narrow-band absorbers are highly needed in the applications for filters, sensors [26] and thermal emission [34,35]. In 2008, Landy et al. [25] presented a narrow-band perfect metamaterial absorber with a single absorption peak and the absorption rate is slight lower 96%. In 2010, Liu et al. [26] presented an infrared perfect absorber which can be used for plasmonic sensor, the FOM* of it is 87. A few years later, Zhao et al. [27] demonstrated an ultra-narrow band absorber consisting of continuous sliver and alumina film. The absorption bandwidth was less than 7 nm and the single peak absorbance reach over 97%. In 2012, Chen et al. [28] presented a dual-band perfect absorber with high absorption rates, and the distance between the two absorption peaks is about 3000 nm. However, the narrow-band absorber with a narrow width between two absorption peaks is rarely reported.

In this work, using the plasmonic analogy of EIR-like effect [29], we present a narrow-band perfect absorber with two absorption peaks based on a second-order plasmonic resonance. Both the two absorption peaks have a near-unity absorption. Due to the width between the two absorption peaks is quite small and the Q-factor of the two absorption peaks is very high, our perfect absorber is a narrow-band absorber and has a great potential to be a filter and plasmonic sensor. Due to that the figure of merit FOM* of two absorption peaks can achieve 319 and 292, respectively, the perfect absorber can be used for a dual-band plasmonic sensor.

Fig. 1 presents the schematic of the perfect absorber, which has three layers, top layer, middle layer and bottom layer. The top layer and the bottom layer are separated by dielectric MgF_2 spacer. The top layer consists of three gold bars, two short gold bars with the same size in both sides and a long gold bar in the middle. The bottom layer is made up of continuous gold film. These structures are deposited on a silica substrate. The lateral displacement of the two short gold bars with respect to the symmetry axis of middle gold bar is defined as s shown in Fig. 1. The incident plane waves are irradiated along the z direction, and the electric field of the incident plane wave is parallel to the long side of the gold bars. The permittivity of gold is described by Drude model with a plasmon frequency ω_p of 1.37×10^{16} rad/s and a collision frequency υ_c of 4.08×10^{13}Hz [26]. The permittivities of MgF_2 and SiO_2 are 1.9 and 2.25, respectively. The numerical simulations are carried out by using a finite integration package (CST Microwave Studio).

At the top layer, the two short gold bars, serving as the bright mode, can be excited by the incident plane wave. The middle gold

* Corresponding author.
E-mail addresses: yqzhang@ybu.edu.cn (Y.Q. Zhang), xrjin@ybu.edu.cn (X.R. Jin).

http://dx.doi.org/10.1016/j.optcom.2016.03.062
0030-4018/

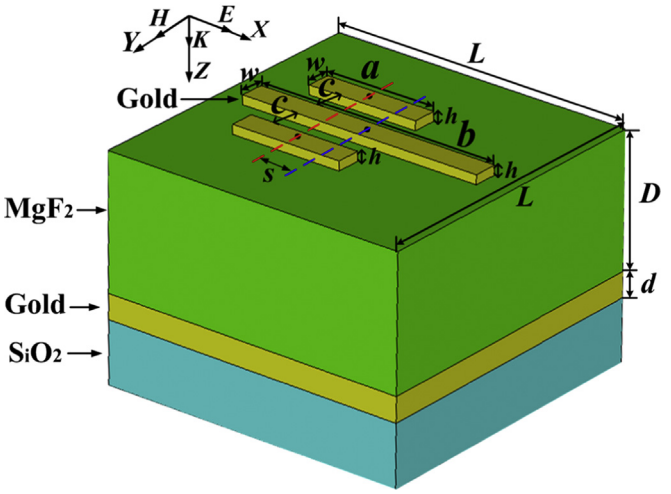

Fig. 1. Schematic of unit cell of the proposed structure. It is a periodic array in x and y directions. The incident radiation is along the z direction, and its polarization is along the x direction, where the geometric parameters are $a=370$ nm, $b=800$ nm, $c=86$ nm, $w=80$ nm, $h=30$ nm, $D=430$ nm, $d=80$ nm and $L=1000$ nm. Displacement s is variable.

bar is not excited by the incident plane wave directly, but excited by the two short gold bars, which results in a second-order resonance mode. The interaction of the bright mode and the dark mode causes the splitting of the plasmon resonance into two new resonances (the bonding and antibonding modes) according to the plasmon-resonance-hybridization scheme [36]. The strength of the coupling between the two resonance modes can be controlled by adjusting the displacement s.

Figs. 2(a) and (b) present the simulated reflection and absorption spectra at optical frequencies with different displacement s, respectively. The black solid, the red dot, the blue short dash and green short dot lines indicate the simulated reflection and absorption spectra for various displacement s from 0 nm to 120 nm with an increase of 40 nm. Fig. 2(b) shows that there is one absorption peak when $s=0$ and the absorption rate is 92.16% at 206.25 THz. This is because that the middle gold bar is not excited, only the two short gold bars are excited by the incident light. Under the circumstances, there is no coupling between the two short gold bars and the middle gold bar. With the increasing of the displacement s, one absorption peak splits into two absorption peaks based on the plasmon hybridization [36], and the low-energy and high-energy peaks get higher. This is owing to that the coupling of the two resonance modes gets stronger with the increasing of displacement s. That is to say, the structure is symmetric when displacement $s=0$. The second-order resonance of middle gold bar cannot be excited due to the electric field excited by two short gold bars is symmetric with respect to the middle gold bar. Therefore, there is no coupling between the short gold bars and the middle gold bar. With the increase of asymmetric degree, the electric field of two short gold bars will excite more electric charges in the middle gold bar. Thus, the strength of coupling between the short gold bars and the middle gold bar (second-order resonance) becomes stronger gradually. When $s=120$ nm, the absorption rates of two absorption peaks are 99.36% (198.47 THz) and 99.51% (207.79 THz), respectively. Furthermore, the quality factors of the perfect absorber at the two absorption peaks are 41.67 (198.47 THz) and 71.42 (207.79 THz), respectively. And the quality factors of two absorption peaks are both much larger than Refs. [26,37]. The width between the two absorption peaks is 9.32 THz. These show that our structure can be used as a plasmonic sensor and a filter. The quality factor is defined as $f_0/\Delta f$, with Δf is the difference value of the frequencies at half maximum of the absorption rate and f_0 is the resonance frequency. Therefore, a narrow dual-band absorber is obtained.

To further support the above arguments, the distributions of the current density and the magnetic filed of the middle gold bar and the gold layer in y-component are shown in Fig. 3. When $s=0$ nm (see Fig. 3(a)), the induced currents only exist in two short gold bars, which means that only two short gold bars are excited. From Fig. 3(b) and (c), we can find that the excited two short gold bars (bright mode) and the middle gold bar (dark mode) are coupled strongly with each other, leading to two new resonance modes (198.47 THz and 207.79 THz), based on the plasmon-resonance hybridization [36]. Also, we can see that the second-order plasmonic resonance mode is excited in middle gold bar, and the antiparallel currents are excited between the middle gold bar and gold layer. Fig. 3(d) shows the y-component of magnetic fields at the x–z plane for the middle gold bar and gold layer when $s=120$ nm, and the strong magnetic fields are confined in MgF_2 layer. Furthermore, the intensity of the two magnetic moments is inequable, they cannot canceled with each other completely. The interaction of the remanent magnetic fields with incident light magnetic field results in nearly zero reflection of the incident light. In addition, the low-frequency (198.47 THz) and the high-frequency (207.79 THz) modes indicate that the induced current is opposite direction and same direction between two short gold bars and middle gold bar, respectively, as shown in Figs. 3(b) and (c). Since the induced-current directions of short gold bars and middle gold bar are same directions in high-frequency, the induced localized magnetic field directions tend to cancel each other. On the contrary, since the induced-current directions of short gold bars and middle gold bar are opposite directions in low-frequency, the induced localized magnetic field directions cannot cancel each other. Therefore, the quality factor of high-frequency is larger than that of low-frequency.

In order to demonstrate our absorber has a great potential in plasmonic sensor, Fig. 4(a) shows the results of a proof-principle simulation which displays the measured reflectance spectra with air ($n=1$) and water ($n=1.312$) on the sample surface when $s=120$ nm. From Fig. 4(a), there is a red-shift of the reflectance curve for water compared with that for air. A figure of merit FOM* is defined as $FOM^* = \max|[dI(\lambda)/dn(\lambda)]/I(\lambda)|$ [37]. The plasmonic absorber sensor detects a relative intensity change of $dI(\lambda)/I(\lambda)$ at a

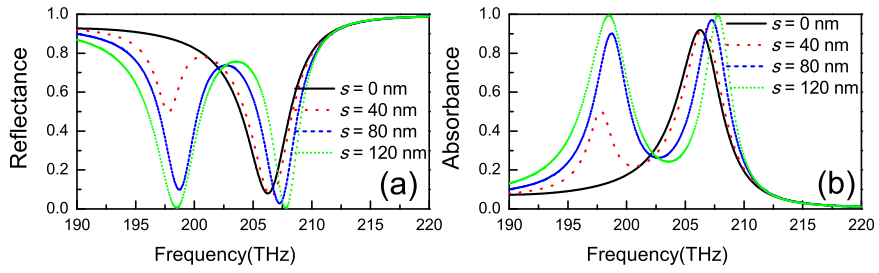

Fig. 2. Simulated reflectance (a) and absorbance (b) spectra with different displacement s. (For interpretation of the references to color in this figure, the reader is referred to the web version of this paper.)